A polymer scaffold binder structure for high capacity silicon anode of lithium-ion battery†

Juchen Guo and Chunsheng Wang*

Received (in Cambridge, UK) 9th September 2009, Accepted 13th January 2010
First published as an Advance Article on the web 27th January 2010
DOI: 10.1039/b918727h

A sodium carboxymethyl cellulose porous scaffold has been obtained using the slurry spray technique as a binder for silicon anodes that demonstrate remarkably improved cycling stability and rate performance.

It has been well recognized that the lithium-ion battery is one of the most promising energy storage technologies to enable a wide range of applications including hybrid electric vehicles (HEV) and electric vehicles (EV) which are essential to reduce the fossil oil dependency. For these particular applications, Li-ion batteries with high power and high energy are critical. However, the graphite anode in current Li-ion batteries cannot fulfil these requirements because of its low specific capacity (372 mAh/g theoretically). In contrast, silicon has very high theoretical specific capacity of 3579 mAh/g.[1] However, the notoriously poor cycle stability due to severe volume expansion/shrinkage during lithium insertion/extraction has obstructed its realization.

A few recent developments in Si anodes, such as Si nano-wires,[2–4] nano-porous structured Si particles[5] and Si anodes using sodium carboxymethyl cellulose (CMC) binder[6–10] have attracted considerable attention. Among these developments, the Si anode with low nano-Si content (28–34 wt%) and high content of CMC binder[10] stood out as a simple procedure with attractive performance. However, the trade off of this technique was that adding more CMC binder and conductive additive lowered the overall anode capacity. Also, a large and continuous irreversible capacity was observed throughout the cycling, because the repeated expansion/shrinkage of Si particles demolished the dense CMC binder structure and cracked the SEI film. In order to alleviate the deformation of the CMC binder during cycling, the authors hereby report a porous CMC scaffold structure as binder for Si anodes (schematic in Fig. 1). The advantage of this scaffold binder is that the intentionally introduced cavities (pores) allow the Si particles to expand without deformation of the electrode structure so that the cycle stability of the Si electrode can be greatly improved. Moreover, the scaffold CMC–Si electrodes can also enhance the rate capability because the porous structure increases ion transport in electrodes and accelerates the charge transfer reaction kinetics by the enhanced surface area.

The CMC scaffold electrodes were prepared using the slurry spray technique (Fig. S1 ESI†). The slurry consisted of 52 wt% Si nano-particles, 12 wt% carbon black, 36 wt% CMC using water as solvent. The slurry was sprayed onto the heated copper foil, and water evaporated instantly upon contact with the copper foil, thus a porous scaffold electrode was formed. The same slurry was used to prepare the conventional Si–CMC electrodes with the slurry casting technique as the comparison. Some CMC scaffold electrodes were prepared using carbon coated Si nano-particles that were obtained *via* emulsion polymerization followed by carbonization (ESI†). The purpose of carbon coating is to enhance the electronic conductivity of the Si nano-particles and to stabilize the SEI film.[11] The carbon coating was confirmed by TEM (Fig. S2 ESI†), and the percentage of carbon was determined to be ~16.0 wt% by energy dispersive X-ray spectroscopy (EDS) (Fig. S3 ESI†). Accordingly, in the preparation of the electrodes using carbon coated Si nano-particles, 52 wt% Si was based on the true Si content.

Nitrogen adsorption measurements have been performed on both the CMC scaffold electrode and the conventional one to obtain their specific surface area, average pore size, and pore size distribution. These results are listed in the table below:

Electrode type	Surface area/m^2 g^{-1}	Mean pore diameter/nm	Total pore volume/cm^3 g^{-1}
Scaffold	28.04	34.6	0.216
Conventional	7.48	64.3	0.111

Fig. 2 shows cumulative pore volume *vs.* pore diameter, inset is the isotherm of N_2 adsorption *vs.* relative pressure. Both samples have broad pore size distribution of which the majority ranges from 50 nm to 120 nm. The CMC scaffold electrode has both higher specific surface area and higher pore

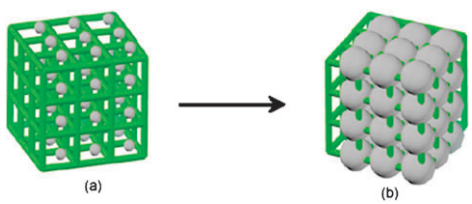

Fig. 1 3D scaffold binder structure: silicon particles are bound in the porous polymer binder scaffold (a). During Li-ion insertion, the scaffold structure is able to accommodate the volume expansion without demolishing the structure (b).

Department of Chemical and Biomolecular Engineering, University of Maryland, College Park, Maryland 20742, USA. E-mail: cswang@umd.edu; Fax: +01 (1) 301-405-9126; Tel: +01 (1) 301-405-0352

† Electronic supplementary information (ESI) available: Experimental details, slurry spray technique schematic, TEM image of carbon coated Si nano-particle and EDS analysis of carbon coated Si nano-particle. See DOI: 10.1039/b918727h

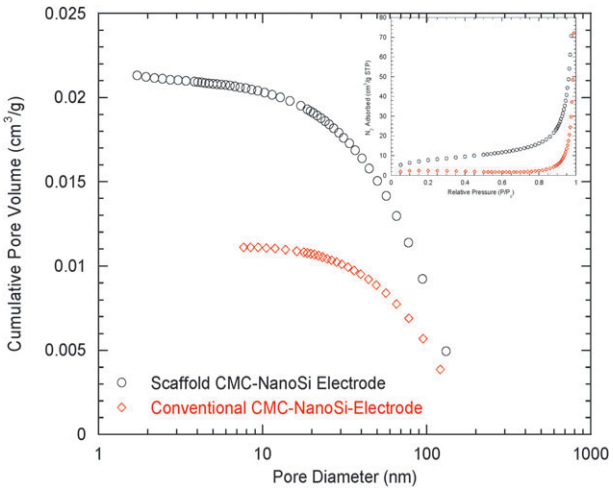

Fig. 2 Surface area and porosity of CMC scaffold electrode and conventional electrode: cumulative pore volume *vs.* pore diameter and N_2 adsorption isotherm.

volume. The structures of the electrodes have also been evaluated using scanning electron microscopy (SEM). Fig. 3 shows the SEM images of the surface and cross-section of the conventional electrode and the CMC scaffold electrode, respectively. It can be observed that the scaffold electrodes have higher porosity.

The CMC scaffold Si electrodes were charged (Li insertion) and discharged (Li extraction) between 1.5 V and 0.0 V at different rates, and their discharge capacity retentions are shown in Fig. 4 (symbols are the capacities and lines are the coulombic efficiencies). The black circles are the cycle life of the conventional CMC–Si electrode made by the slurry casting method. It is clear that the scaffold CMC–NanoSi electrode (blue diamonds) is distinctly superior to the corresponding conventional electrode. Carbon coating on the Si nano-particles (denoted as Scaffold CMC-C/NanoSi) can further enhance the cycling stability of the electrodes. The carbon coated Si nano-particles could retain capacity of 1685 mAh/g (78% capacity retention) after 150 cycles at 250 mA g^{-1} charge/discharge current. The coulombic efficiencies of the CMC scaffold electrodes could reach more than 98% after only a few charge/discharge cycles. The discharge rate capacities of the CMC scaffold–NanoSi electrodes with or without carbon coating on Si are shown as the inset of Fig. 4. The electrodes were charged at the same rate, 0.05 C (100 mA g^{-1}), and discharged at 0.05 C, 0.1 C, 0.2 C, 0.5 C, 1 C and 1.5 C, respectively. At each C rate, the electrodes were cycled at least in triplicate. It can be seen that the electrodes with either Si nano-particles or carbon coated Si nano-particles could retain great capacity even at high discharge rates. At 1.5 C (3000 mA g^{-1}), the CMC scaffold–NanoSi electrode could provide discharge capacity of 1800 mAh/g (75% of the capacity at 0.05 C). The similar rate performance of these two types of Si nano-particles (with or without carbon coating) demonstrated that the electronic conductivity of the CMC scaffold (mixed with carbon) was sufficient for a high discharge rate such as 1.5 C. The porous structure of the scaffold CMC–Si electrodes could facilitate the lithium ion transport in the electrodes and accelerate the charge transfer reaction kinetics.

To better understand the mechanism of the improvement of cycling stability by carbon coating, CMC scaffold–NanoSi electrodes with and without carbon coating were disassembled in an argon filled glove box after 63 charge/discharge cycles, and the surface morphologies of these two electrodes were evaluated using SEM as shown in Fig. 5. Compared to the

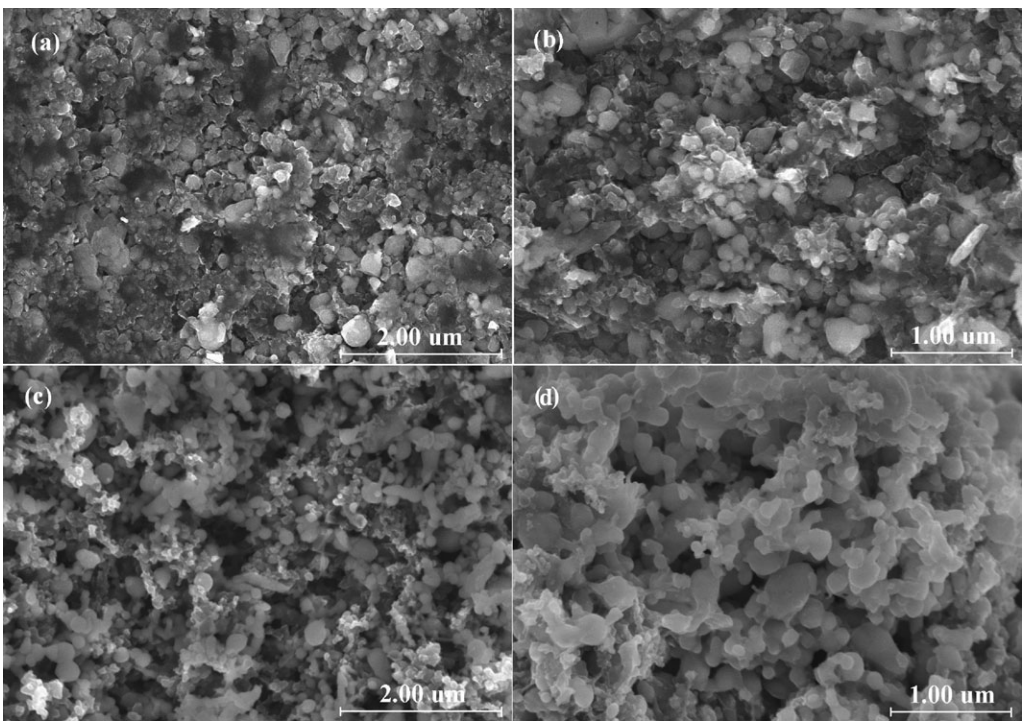

Fig. 3 Surface (a) and cross-section (b) of control CMC–Si electrode; surface (c) and cross-section (d) of scaffold CMC–Si electrode.

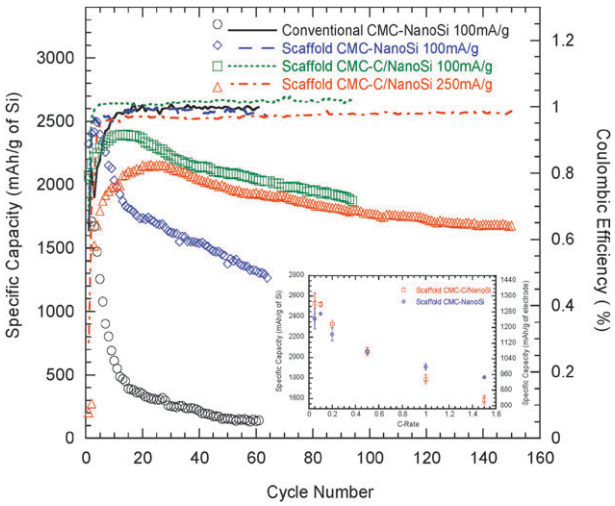

Fig. 4 Cycle stabilities of Si nano-particle electrodes with CMC scaffold binder.

corresponding surface morphologies before cycling shown in the insets in Fig. 5, the porous morphology of the CMC scaffold–NanoSi electrode (without carbon coating on Si) was almost entirely covered by the SEI film, while the porous structure of the CMC scaffold-C/NanoSi electrode can still be obseved. A recent article by Yen and coworkers[11] suggested that the carbon coating on the Si surface could largely reduce the formation of the SEI film. The cycle stability test results and the SEI film images in Fig. 4 and 5 agreed with Yen's conclusion very well.

The concept of scaffold binder structure has also been tested in the CMC scaffold electrode made of micron-sized Si powder (average size ~2 μm). The cycle stability of the CMC scaffold micron-Si anode is shown in Fig. 6. At 250 mA g^{-1} charge/discharge rate, the CMC scaffold–MicronSi electrode (red triangle symbols) can retain capacity of 930 mAh/g after 85 cycles, which is much higher than the conventional

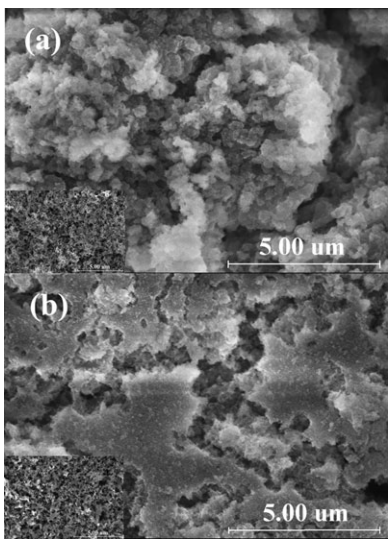

Fig. 5 Surface morphology of a scaffold CMC-C/NanoSi electrode after 63 charge/discharge cycles (a); surface morphology of a scaffold CMC–NanoSi electrode after 63 charge/discharge cycles (b).

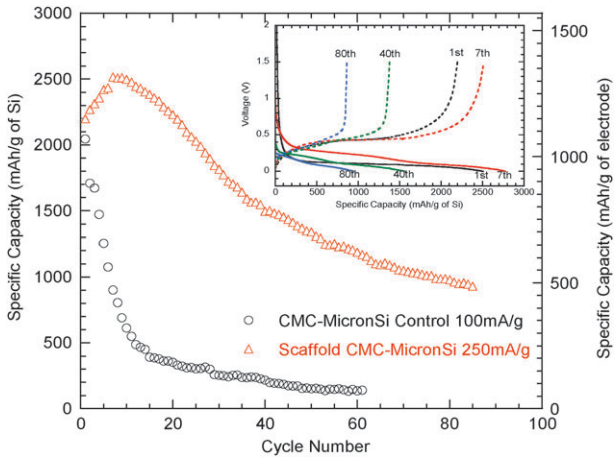

Fig. 6 Cycle stabilities of Si micron-particle electrodes with CMC scaffold binder.

electrode (black circle symbols) made by the slurry casting technique with the same composition. It is also worth mentioning that the irreversible capacity of the CMC scaffold micron-Si electrodes in the first charge/discharge cycle is only 12.4% as shown in the inset of Fig. 6.

In conclusion Si nano-particle electrodes with CMC scaffold binder structure showed high energy density, power density and superb cycle stability, because the porous CMC scaffold can accommodate more volume changes of Si and enhance the lithium ion transport in the electrodes, as well as being able to improve the electrochemical reaction kinetics. The Si content, porosity and pore size in the CMC scaffold binder will be optimized in future studies. Different CMC polymers and preparation conditions (pH value) will also be investigated.

Financial support from the University of Maryland is gratefully acknowledged. The authors also thank Dr Li-Chung Lai at the University of Maryland Nanoscale Imaging Spectroscopy and Properties Laboratory for his help with the TEM characterization. The authors are grateful to Dr Chengsong Ma and Dr Kamen Nechev at Saft America Inc. for their help with the BET test.

Notes and references

1 M. N. Obrovac and L. Christensen, *Electrochem. Solid-State Lett.*, 2004, **7**, A93.
2 C. K. Chan, H. Peng, G. Liu, K. Mclwrath, X. F. Zhang, R. A. Huggins and Y. Cui, *Nat. Nanotechnol.*, 2008, **3**, 31.
3 B. Laik, L. Eude, J.-P. Pereira-Ramos, C. S. Cojocaru, D. Pribat and E. Rouviere, *Electrochim. Acta*, 2008, **53**, 5528.
4 K. Peng, J. Jie, W. Zhang and S.-T. Lee, *Appl. Phys. Lett.*, 2008, **93**, 033105.
5 H. Kim, B. Han, J. Choo and J. Cho, *Angew. Chem., Int. Ed.*, 2008, **47**, 10151.
6 W.-R. Liu, M.-H. Yang, H.-C. Wu, S. M. Chiao and N.-L. Wu, *Electrochem. Solid-State Lett.*, 2005, **8**, A100.
7 H. Buqa, M. Holzapfel, F. Krumeich, C. Veit and P. Novak, *J. Power Sources*, 2006, **161**, 617.
8 J. Li, R. B. Lewis and J. R. Dahn, *Electrochem. Solid-State Lett.*, 2007, **10**, A17.
9 N. S. Hochgatterer, M. R. Schweiger, S. Koller, P. R. Raimann, T. Wöhrle, C. Wurm and M. Winterc, *Electrochem. Solid-State Lett.*, 2008, **11**, A76.
10 S. D. Beattie, D. Larcher, M. Morcrette, B. Simon and J.-M. Tarascon, *J. Electrochem. Soc.*, 2008, **155**, A158.
11 Y.-C. Yen, S.-C. Chao, H.-C. Wu and N.-L. Wu, *J. Electrochem. Soc.*, 2009, **156**, A95.

